Molecular Crystals and Liquid Crystals

Publication details, including instructions for authors and subscription information:
http://www.tandfonline.com/loi/gmcl20

Rheo-Nmr and Numerical Study of the Nematodynamics in Cylindrical Couette Geometry

Laura Orian [a], Gabriel Feio [a], Alain Veron [a], Assis Farinha Martins [a] & Antonino Polimeno [b]

[a] Dep. Ciência dos Materiais, Faculdade de Ciências e Tecnologia, Universidade Nova de Lisboa, Caparica, 2829-516, Portugal

[b] Dip. Chimica Fisica 'A. Miolati', Università degli Studi di Padova, Via Loredan 2, Padova, 35100, Italia

Version of record first published: 18 Oct 2010

To cite this article: Laura Orian, Gabriel Feio, Alain Veron, Assis Farinha Martins & Antonino Polimeno (2003): Rheo-Nmr and Numerical Study of the Nematodynamics in Cylindrical Couette Geometry, Molecular Crystals and Liquid Crystals, 394:1, 63-75

To link to this article: http://dx.doi.org/10.1080/15421400390193675

Mol. Cryst. Liq. Cryst., Vol. 394, pp. 63–75, 2003

ISSN 1542-1406 print/1563-5287 online
DOI: 10.1080/15421400390193675

RHEO-NMR AND NUMERICAL STUDY OF THE NEMATODYNAMICS IN CYLINDRICAL COUETTE GEOMETRY

Laura Orian, Gabriel Feio, Alain Veron, and Assis Farinha Martins
Dep. Ciência dos Materiais, Faculdade de Ciências e Tecnologia, Universidade Nova de Lisboa, 2829-516 Caparica, Portugal

Antonino Polimeno
Dip. Chimica Fisica 'A. Miolati', Università degli Studi di Padova, Via Loredan 2, 35100 Padova, Italia

A numerical study of the hydrodynamics of nematic liquid crystals in cylindrical Couette geometry is presented, based on Leslie-Ericksen theory. The aim of this study is to interpret the director dynamics observed in Rheo-NMR experiments, where the sample (lyotropic cholesteric system PBLG/m-cresol 14%) is subjected to viscous, elastic and magnetic torques. When analysing the macroscopic response of the liquid crystal polymer to the azimuthal Couette flow, competing with the effect of the strong magnetic field applied perpendicular to the shear plane in the NMR set-up, we observe the existence of a steady state characterised by a distribution of director orientations neither parallel to the field nor in the shear plane. We show that this behaviour requires the occurrence of an instability, like the director analogue of Taylor cells, associated to a secondary flow. A proper modelling of the velocity profile allows us to interpret satisfactorily the main features of the experimental data.

Keywords: Leslie-Ericksen equations; couette geometry; nematic liquid crystal

INTRODUCTION

In the rationalisation and full understanding of rheological behaviour of low molecular weight nematogens and nematic polymers, some interesting

This work was partly supported by the European Commission under TMR contract FMRX-CT97-0121 and by the Italian Ministry for Universities and Scientific and Technological Research (PRIN "Cristalli Liquidi").

problems remain still largely unexplored, due to the complexity of the non-linear response of these viscoelastic media to the applied shear stress in a great variety of experimental situations.

In the early sixties Ericksen formulated the theory to describe the macroscopic response of a uniaxial liquid to a velocity gradient [1]. Leslie applied it to the nematic fluids, introducing the elastic torque [2]. The fundamental aspect is that simple shear exerts a torque on the director **n**. Roughly two basic situations arise according to the sign of α_3/α_2 where α_2 and α_3 are two Leslie viscosities. When $\alpha_3/\alpha_2 > 0$ the director aligns with a direction close to the streamline (this is the *flow alignment* regime) while in the opposite case the director continuously rotates (this is the *tumbling* regime). However, often more complex director patterns arise both in aligning and tumbling systems [3], resulting from a subtle competition between the viscous, the elastic (related to the anchoring at the walls) and eventually the magnetic (or electric) torques that makes the flow unstable. Two types of shear-induced instabilities have been observed and analysed in nematics: the homogeneous distortion and the rolling-like regimes [4]. Pieranski and Guyon studied and interpreted the formation of homogeneous distortions in simple shear flow of a nematic film between two glass plates with carefully imposed boundary conditions [5]. Manneville and Dubois-Violette formulated a bi-dimensional hydrodynamic model and determined with good accuracy both homogeneous and rolling instability thresholds for a nematic sheared in planar geometry [6]. Many studies about the response of nematic samples to simple shear flow in parallel plate geometry are available. Koch and co-workers predicted from symmetry considerations the shape of the threshold curves, fixing the boundaries between different flow regimes occurring in a homeotropic nematic submitted to a periodical shear [7]. Barratt and Manley developed an accurate method to calculate the shear rate thresholds for homogeneous and roll type instabilities in nematics subjected to simple shear flow [8]. The response to Couette flow has also been investigated: Cladis and Torza focused their attention in Taylor-Couette instabilities in nematic liquid crystals [3,9]; Barratt and co-workers proposed a linear instability analysis for thin nematic layers subjected to Couette flow [10].

A methodology for solving nematodynamics equations has been developed in the last three years by Polimeno, Martins and coworkers, who applied it to study systematically the director dynamics in different geometries in order to interpret rheological and magneto-rheological experiments [11–16].

The purpose of this work is to investigate the effect of rolling-like instabilities in Couette flow on the time evolution of director patterns. The assumption of a secondary cellular flow may be justified by experimental evidences and stability analysis presented in literature for analogous

systems [10,17]. The numerical results are used to interpret the main features of a set of Rheo-NMR spectra obtained with PBLG (poly-L-benzyl-glutamate)/m-cresol 14%. The Rheo-NMR methodology, combining NMR techniques with traditional rheometry, has proved to be a powerful tool to study both at molecular and macroscopic levels the properties of complex fluids [18]. In particular, it is possible to obtain relevant information about the molecular orientation, viscoelastic properties and dynamics of a liquid crystalline system under shear conditions and in the presence of a strong, static, magnetic field [19,20].

The delicate competition of viscous, elastic and magnetic torques, acting on a uniaxial liquid crystal produce a spatially complex, time-dependent, orientation pattern of the director, not fully understood. This situation provides a framework where the Rheo-NMR approach is particularly well suited as a valuable technique, allowing to apply theoretical hydrodynamic models of nematic liquid crystals and corresponding numerical analysis to the interpretation of experimental observations [14].

The director dynamics has been followed experimentally using a Couette mini-rheometer inserted in the superconducting magnet of the NMR spectrometer and coupled to the NMR probe head. Adding traces of deuterated benzene as a NMR probe, ^{2}H-NMR technique can be used to follow the macroscopic response of the sample during and after the rheological excitation imposed by the applied shear. The doublet splitting, resulting from the partial average of the quadrupolar interaction in the anisotropic uniaxial medium, provides information on the director orientation with respect to the magnetic field, which has been chosen parallel to the Couette cell axis in the set-up used for this work.

The director dynamics is interpreted in the framework of Leslie-Ericksen theory [21], adopting a Newtonian velocity field, in order to simplify the numerical treatment, but keeping the full three-dimensional description of the director field and the Couette geometry. The time evolution of the director pattern is mainly governed by the action of three torques: the magnetic torque, the viscous torque due to the imposed Couette shear flow and the elastic torque. Finally, we take into account the effect of a secondary flow, related to the presence of Taylor rolling-like instabilities formed in these highly viscous samples at low values of the Ericksen number [22,23]. Modulating the intensity of this perturbation we can observe damping of the usual predicted tumbling and the occurrence of a steady state characterised by a director alignment close to the shear plane, that is in agreement with the experimental results.

The paper is organised as follows: in the two first sections the Rheo-NMR experiment and the hydrodynamic model are presented and in the last section the experimental and theoretical results are compared and discussed.

THE RHEO-NMR EXPERIMENTS

The Rheo-NMR experiments were performed on a lyotropic cholesteric PBLG/m-cresol (14%) system under shear flow in a Couette mini-rheometer fitted in the NMR probe head. The nuclear spin response of a deuteriated benzene probe, added to the sample in minute amounts (1%), was monitored in two distinct situations: i) under shear flow, when a constant rotational velocity was applied to the inner cylinder of the Couette rheometer, at different shear rates, until a stationary response has been reached; ii) when that rotation was suddenly stopped and the system underwent a stress relaxation process until the initial state was completely restored.

The deuterium observation has been chosen because the quadrupolar coupling of this nucleus is a convenient tool for investigating the orientational ordering of the C_6D_6 probe, which is expected to reflect directly the director orientational distribution and dynamics in the liquid crystalline media.

The Couette rheometer is made of two main parts, a Couette cell and a cover that keeps all the set-up fixed to the Teflon basis of the probe head. Two concentric cylinders with axis parallel to the magnetic field direction compose the rheometer cell, which is adjusted within the rf coil to optimize the filling factor. The appropriate resonant circuits for rf excitation and detection, tuned at 46,073 MHz, were adapted to the insert of a commercial Bruker NMR probe. The outer cylinder is fixed and the inner one is coupled to the external step motor by an appropriate non-magnetic rigid shaft. The cylinders, made of Vespel, are about 4 cm height but only the central part, with a length of 2 cm, is inside the detection zone of the NMR coil, in order to minimize the end effects of the shear flowing fluid in the Couette cell. The outside diameter of the inner cylinder is 8 mm and the inside diameter of the fixed outer cylinder is 9 mm, which gives an annular gap of 0.5 mm, between the bounding walls, for the fluid motion. The total sample volume used in this device is less than 1cc.

The Rheo-NMR experiments were performed, at 303 K, at different shear rates. However, in this study, only a shear rate of $20\,s^{-1}$ is considered. The deuterium spectra were obtained with a quadrupolar echo sequence, first under shear flow, for a time period necessary to impose to the sample at least 400 units of deformation, and then, after stopping the applied rate of strain, when the system is allowed to relax back to equilibrium, for a period of approximately 45 minutes. In the shear flow regime 15 spectra were recorded, at different time intervals. The first acquisition was obtained 10 s immediately after the starting of the rotation, in order to detect any overshoot effect preceding a steady shear response. In the relaxation regime 18 spectra were recorded, also at variable time intervals

until no more changes in the line shapes were observed (Fig. 1). The first of the whole set of 34 spectra is an equilibrium spectrum, recorded just before the start of the shearing, when the sample has fully relaxed for at least 60 minutes from any previous Rheo-NMR measurement. Each experiment accounts for one scan regarding each of the 34 spectra, recorded in one single run in a 2D sequential file. In order to obtain a reasonable signal to noise ratio in the spectra, a total of 12 experiments were performed, corresponding to 12 addictive scans of the deuterium time domain response (FID).

The deuteron NMR Fourier Transform spectra obtained in the above experiments consist in a quadrupolar doublet with a line splitting that is highly sensitive to the director orientation $\Theta(t)$ of the liquid crystalline sample with respect to the magnetic field of the spectrometer. The action of any force field (magnetic, viscous or elastic) inducing an alignment of the director can therefore be investigated by analyzing the NMR line shape of an appropriately labelled probe dispersed in the anisotropic system. The basic relationship between the line splitting in the spectra, $\delta v(t)$, and the director orientation is given by:

$$\delta v = \delta v_0 \frac{1}{2}\left(3\,cos^2\,\Theta(t) - 1\right) \tag{1}$$

where δv_0 is the line splitting measured in the equilibrium spectrum. If the system is not spatially homogeneous, the director orientation depends also

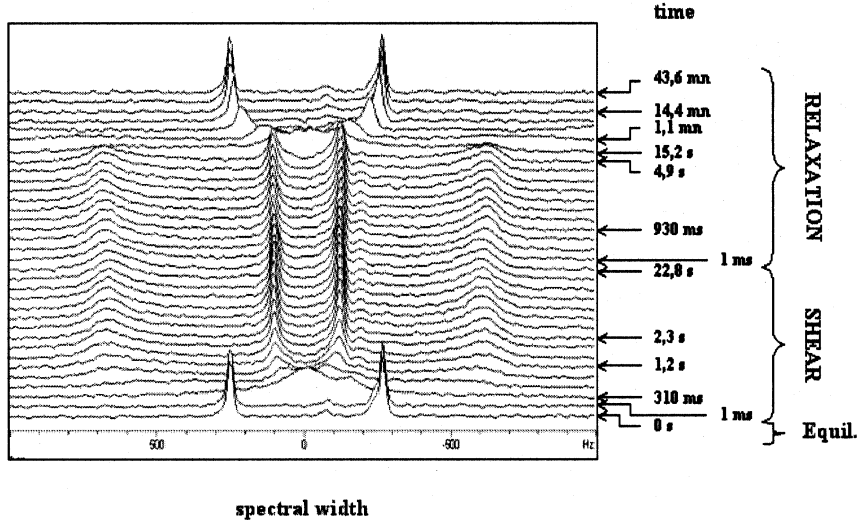

FIGURE 1 Rheo-NMR spectra at shear rate $20\,s^{-1}$.

on the spatial coordinates, $\Theta(\mathbf{r}, t)$, and the shape of each of the doublet lines accounts as well for the director spatial distribution. In this situation the splitting should be interpreted as a spatial average of the director distribution in the sample, with respect to the magnetic field, under any of the induced physical regimes: equilibrium, flow or relaxation.

In the equilibrium state the director was uniformly aligned with the magnetic field of the spectrometer and the deuterium spectrum of the benzene probe exhibits a well-defined doublet of sharp lines, providing an accurate measurement of $\delta\upsilon_0$. Then the constant rotational velocity was applied to the inner cylinder of the Couette rheometer until a stationary response was observed. Almost immediately after the applied shear at 20 s^{-1}, the sample produced a spatially complex time-dependent orientation pattern, which is well reflected by the line-shape of the NMR spectra recorded during the initial 3 s, to which it follows a steady state with a constant doublet splitting with value $\delta\upsilon$ (function of the applied shear rate), characterizing a stationary spatial distribution of director orientations neither parallel to the field nor in the shear plane. When the rotation is suddenly stopped, the system relaxes back to the homogeneously oriented configuration imposed by the magnetic field.

In this work we analyse only the quadrupolar doublet splitting of the NMR spectra, recorded in the time period corresponding to the steady state response of the PBLG/m-cresol (14%) liquid crystalline system, under a constant shear rate of $20\,s^{-1}$.

THE HYDRODYNAMIC MODEL

A cylindrical reference system is chosen, defined by the three orthogonal vectors $(\mathbf{e}_r, \mathbf{e}_\vartheta, \mathbf{e}_z)$ (Fig. 2). The calculation is made for Taylor-like cells associated with the secondary flow as defined in Figure 2 and below in this section. A point inside the cell is thus identified by the set (r, ϑ, z), with $r_i \leq r \leq r_o$, $0 \leq \vartheta \leq 2\pi$ and $0 \leq z \leq d$ where r_i and r_o denote respectively the radius of the inner and the radius of the outer cylinder and $d = r_o - r_i$. A full three-dimensional description of the director is taken, i.e. $\mathbf{n}(r, \vartheta, z, t) \equiv (n_r(r, \vartheta, z, t), n_\vartheta(r, \vartheta, z, t), n_z(r, \vartheta, z, t))$.

Newtonian behaviour is assumed for the velocity; that is the velocity field is obtained analytically solving Navier-Stokes equations for cylindrical Couette flow [24]. Neglecting inertial terms, the director equation is obtained from the torque balance equation

$$\mathbf{k}^e + \mathbf{k}^m + \mathbf{k}^{\mathbf{v}} = 0 \tag{2}$$

with $\mathbf{k}^e$ the elastic torque, $\mathbf{k}^m$ the magnetic torque and $\mathbf{k}^v$ the viscous torque. The elastic torque is given by:

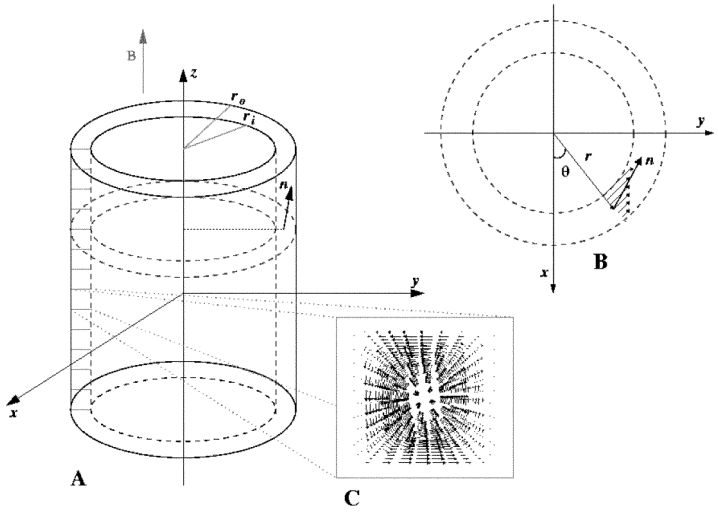

FIGURE 2 Geometrical set-up: three-dimensional Couette scheme (A), horizontal section (B) and vector velocity plot of the rolling cell (C).

$$\mathbf{k}^e = \mathbf{n} \times \left[div\left(\frac{\partial W}{\partial \nabla \mathbf{n}}\right) - \frac{\partial W}{\partial \mathbf{n}} \right] \tag{3}$$

where W is the Frank free elastic energy density:

$$W = \frac{1}{2}K_{11}(\hat{\nabla} \cdot \mathbf{n})^2 + \frac{1}{2}K_{22}(\mathbf{n} \cdot \hat{\nabla} \times \mathbf{n})^2 + \frac{1}{2}K_{33}(\mathbf{n} \times \hat{\nabla} \times \mathbf{n})^2 \tag{4}$$

Introducing the spherical approximation ($K_{11} = K_{22} = K_{33} = K$), Eq. (3) is simplified:

$$\mathbf{k}^e = K\mathbf{n} \times \nabla^2 \mathbf{n} \tag{5}$$

The magnetic torque reads:

$$\mathbf{k}^m = \chi_a(\mathbf{n} \times \mathbf{H})(\mathbf{n} \cdot \mathbf{H}) \tag{6}$$

where χ_a is the diamagnetic anisotropy and $\mathbf{H} \equiv (0, 0, H)$ is the magnetic field. The viscous torque is given by:

$$\mathbf{k}^v = -\mathbf{n} \times [\gamma_1(\dot{\mathbf{n}} - \mathbf{\Omega}\mathbf{n}) + \gamma_2 \mathbf{A}\mathbf{n}] \tag{7}$$

where the superposed dot denotes the material time derivative $\dot{\mathbf{n}} = \partial \mathbf{n}/\partial t + \mathbf{v} \cdot \nabla \mathbf{n}$. The following tensors appear in Eq. (6):

$$\mathbf{\Omega} := \frac{1}{2}\left[\nabla \mathbf{v} - (\nabla \mathbf{v})^T\right] \tag{8}$$

$$\mathbf{A} := \frac{1}{2}\left[\nabla\mathbf{v} + (\nabla\mathbf{v})^T\right] \tag{9}$$

The two viscosities γ_1 and γ_2 can be expressed as linear combinations of Leslie viscosities, $\gamma_1 = \alpha_3 - \alpha_2$ and $\gamma_2 = \alpha_2 + \alpha_3$. The velocity field for a Newtonian cylindrical Couette flow has a single non-null component v_ϑ that, when only the inner cylinder rotates with the angular velocity ω_i, can be written as:

$$v_\vartheta = B\left(\frac{A}{r} - Cr\right) \tag{10}$$

with $A = \omega_i r_i^2 r_o^2$, $B = \left(r_o^2 - r_i^2\right)^{-1}$ and $C = \omega_i r_i^2$ [24]. It should be noted that the velocity profile (10) associated with a director uniformly aligned parallel to the vorticity axis is actually an exact solution of the Leslie-Ericksen equations [10]. Accordingly it may be seen as a good first approximation.

Given that the director is a unit vector, it is convenient to introduce the two polar angles Θ and Φ (see Fig. 1) in such a way that the director components read:

$$n_r = sin\,\Theta\,cos\,\Phi \quad n_\vartheta = sin\,\Theta\,sin\,\Phi \quad n_z = cos\,\Theta \tag{11}$$

Using the definitions (11), after some algebraic manipulations, the system of equations (2) becomes equivalent to:

$$\gamma_1 \frac{\partial\Phi}{\partial t} = \frac{1}{r^2}\left[AB(\gamma_2\,cos\,2\Phi - \gamma_1) - \gamma_1 B\left(A - Cr^2\right)\frac{\partial\Phi}{\partial\vartheta}\right] + \mathcal{K}_\Phi^e \tag{12}$$

$$\begin{aligned}\gamma_1 \frac{\partial\Theta}{\partial t} = &\frac{1}{r^2}\left[\frac{\gamma_2}{2}AB\,sin\,2\Phi\,sin\,2\Theta - \gamma_1 B\left(A - Cr^2\right)\frac{\partial\Theta}{\partial\vartheta}\right] + \mathcal{K}_\Theta^e \\ &- \frac{\chi_a H^2}{2}sin\,2\Theta\end{aligned} \tag{13}$$

where the terms coming from the elastic torque read:

$$\begin{aligned}\mathcal{K}_\Phi^e = K\Big\{&sin\,\Phi\lfloor sin\,\Theta\,sin\,\Phi\left(\nabla^2\mathbf{n}\right)_z - cos\,\Theta\left(\nabla^2\mathbf{n}\right)_\vartheta\rfloor \\ &- cos\,\Phi\left[cos\,\Theta\left(\nabla^2\mathbf{n}\right)_r - sin\,\Theta\,cos\,\Phi\left(\nabla^2\mathbf{n}\right)_z\right]\Big\}\end{aligned} \tag{14}$$

$$\mathcal{K}_\Theta^e = K\,sin\,\Theta\lfloor cos\,\Phi\left(\nabla^2\mathbf{n}\right)_\vartheta - sin\,\Phi\left(\nabla^2\mathbf{n}\right)_r\rfloor \tag{15}$$

where $\left(\nabla^2\mathbf{n}\right)_i$ denotes the Laplacian of the director components in cylindrical coordinates.

The system of Eqs. (12–13) can be solved numerically using a finite difference scheme on a three-dimensional cylindrical grid [25].

To investigate the effects of rolling instabilities, we consider a secondary flow characterised by non-null v_r and v_z components. This secondary flow

describes rolls whose section lies in the rz plane and such that the velocity field lines draw approximately a thoroid coaxial with the Couette cell. The perturbation must satisfy incompressibility and boundary conditions:

$$\frac{\partial v_r}{\partial r} + \frac{1}{r}\left(\frac{\partial v_\vartheta}{\partial \vartheta} + v_r\right) + \frac{\partial v_z}{\partial z} = 0 \tag{16}$$

$$v_r(r_i, z) = v_r(r_o, z) = 0, \quad v_z(r_i, z) = v_z(r_o, z) = 0 \tag{17}$$

It is straightforward to demonstrate that the above criteria are verified choosing $v_r = (-F(r)/r)(dI(z)/dz)$ and $v_z = (1/r)(dF(r)/dr)I(z)$ where $F(r)$ is a function of r subjected to the restrictions $F(r_i) = F(r_o) = 0$ and $(dF(r)/dr)_{r=r_i} = (dF(r)/dr)_{r=r_o} = 0$, and $I(z)$ is an arbitrary function of z. Thus we can write Eq. (2) in the following general way:

$$\begin{aligned}\gamma_1 \frac{\partial \Phi}{\partial t} = \frac{1}{2r^2}\Bigg\{ & 2\gamma_2\left[AB\cos 2\Phi + \sin 2\Phi\left(2F(r) - r\frac{dF(r)}{dr}\right)\frac{dI(z)}{dz}\right] \\ & + \sin\Phi\cot\Theta\left[(\gamma_1+\gamma_2)I(z)\left(-\frac{dF(r)}{dr} + r\frac{d^2F(r)}{dr^2}\right)\right. \\ & \left. + (\gamma_1-\gamma_2)rF(r)\frac{d^2I(z)}{dz^2}\right] - 2\gamma_1 \\ & \times\left[AB + rI(z)\frac{dF(r)}{dr}\frac{\partial\Phi}{\partial z} + B(A - Cr^2)\frac{\partial\Phi}{\partial\vartheta} + \right. \\ & \left. - rF(r)\frac{dI(z)}{dz}\frac{\partial\Phi}{\partial r}\right]\Bigg\} + \mathcal{K}^e_\Phi \end{aligned} \tag{18}$$

$$\begin{aligned}\gamma_1 \frac{\partial \Theta}{\partial t} = -\frac{1}{4r^2}\Bigg\{ & -\gamma_2 \sin 2\Theta\left[2AB\sin 2\Phi + \left(r(3+\cos 2\Phi)\frac{dF(r)}{dr}\right.\right. \\ & \left.\left. - 2\cos 2\Phi F(r)\right)\frac{dI(z)}{dz}\right] - 2\gamma_2 r\cos\Phi\cos 2\Theta F(r)\frac{d^2I(z)}{dz^2} \\ & + 2I(z)\left[\cos\Phi(\gamma_1 + \gamma_2\cos 2\Theta)\left(-\frac{dF(r)}{dr} + r\frac{d^2F(r)}{dr^2}\right)\right. \\ & \left. + 2\gamma_1 r\frac{dF(r)}{dr}\frac{\partial\Theta}{\partial z}\right] + 2\gamma_1\left[2B(A - Cr^2)\frac{\partial\Theta}{\partial\vartheta}\right. \\ & \left.\left. + rF(r)\left(\cos\Phi\frac{d^2I(z)}{dz^2} - 2\frac{dI(z)}{dz}\frac{\partial\Theta}{\partial r}\right)\right]\Bigg\} + \\ & - \frac{\chi_a H^2}{2}\sin 2\Theta + \mathcal{K}^e_\Theta \end{aligned} \tag{19}$$

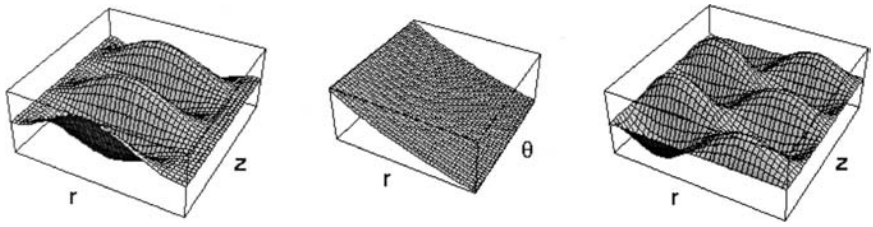

FIGURE 3 Plots of the velocity components (v_r, v_ϑ, v_z).

To model a *roll*, we have chosen the following particular expressions for $F(r)$and $I(z)$:

$$F(r) = d^2\Omega_r \, sin^2\left[q\left(\frac{\pi}{d}\right)(r - r_i)\right] \tag{20}$$

$$I(z) = \frac{d}{\pi} sin\left(\frac{\pi z}{d}\right) \tag{21}$$

where Ω_r is a frequency and q is an integer indicating the number of rolls in the gap. For our purposes we set $q = 1$. We have chosen the same periodicity along r and z, corresponding to the Couette gap. This is a good approximation, since experimentally it has been observed that the roll section is a square with smooth angles [3]. Besides an interesting feature of the cellular pattern is the change in their cross section with increasing shear. At low shear rate the cross section is nearly square; then it becomes closer to a rectangular shape by remaining constant in the r direction and shrinking in the z direction: the cell wavelength decreases with increasing shear. When it becomes so small that the mechanical instabilities associated with the rotation of the inner cylinder or other fluctuations cause them to overlap, disclination threads nucleate and grow around the inner cylinder. The observations end in director turbulence. In Figure 3 the three velocity components (v_r, v_ϑ, v_z) are plotted separately.

RESULTS AND DISCUSSION

The dynamic behaviour of the director field has been studied both in absence and in presence of rolling instabilities. The parameters employed in the simulations are reported in Table 1.

Before shearing, the strong magnetic field aligns the director parallel to the vorticity axis. However, due to thermal fluctuations a slight tilt of the director towards the shear plane is considered. Strong anchoring boundary conditions are chosen for the director at the walls (alignment along z

TABLE 1 Physical Constants Referring to PBLG/m-Cresol 14% System

Couette radii (cm)	0.40, 0.45
Density (g cm^3)	1.000
Viscosity coefficients (Poise)	−3280, −4470, 130, 1420, 2860, −1490
Average elastic constant (dyne)	10^{-7}
Magnetic field (Gauss)	70456
Magnetic anisotropy	7.52×10^{-9}

axis); periodical boundary conditions are imposed along the ϑ and z directions.

In presence of simple Couette flow the director exhibits tumbling behaviour, soon damped by the magnetic torque that tends to align the director back to its initial state of orientation along z. In Figure 4 the contour plots represent the time evolution of the axial director component n_z along the radial coordinate, using a grey colour scale to describe the intermediate orientations between white corresponding to alignment with the magnetic field and black corresponding to a state in which the director lies in the shear plane. The shear rate is $1 s^{-1}$. The band structure has a periodicity of about 20 s, corresponding to the tumbling period; it persists in absence of magnetic field (Fig. 4a), but is destroyed completely after 120 s when the field is present and aligns the director (Fig. 4b). It follows that it is impossible to account for a macroscopic steady state with the

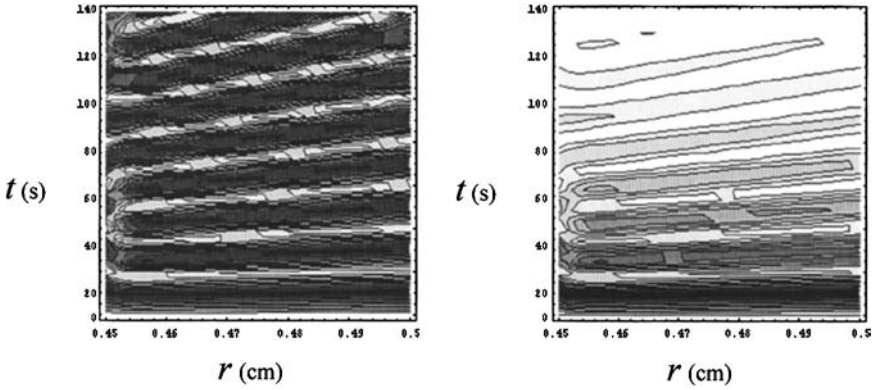

FIGURE 4 Time evolution of the axial director component n_z along the radial coordinate at a shear rate of $1 s^{-1}$, without secondary flow, in absence (a) and in presence (b) of the external magnetic field. (white: the director is parallel to the vorticity axis, black: the director lies in the shear plane).

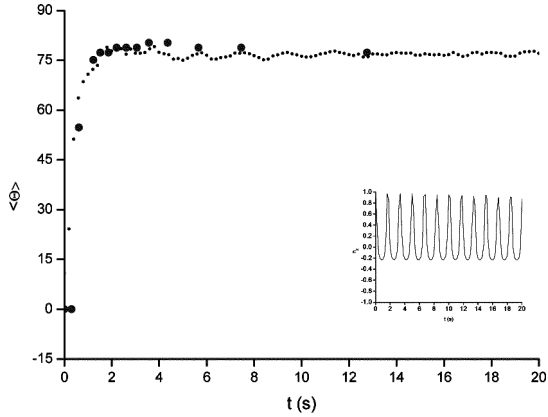

FIGURE 5 Time evolution of the average director orientation with respect to the magnetic field: experimental values (circles) and simulation results (dots). In the lower right corner the time evolution of n_z in the middle of the roll is represented.

director oriented close to the shear plane as clearly evidenced by Rheo-NMR data. For this reason it seems necessary to consider a secondary shear flow.

When a secondary shear flow modelled by Eqs. (18–21) is taken into account, a completely different behaviour occurs. In this case, the director stabilises in a direction intermediate between the vorticity axis and the shear plane in agreement with experiment. From the doublet splittings in the NMR spectra we get information about the orientation of the director with respect to the magnetic field axis. In Figure 5 the angle Θ measured in the spectra (circles) taken during shear and its average value calculated numerically (dots) are compared. The applied shear rate is $20\,s^{-1}$; the value of Ω_r is $1s^{-1}$; a grid of $20\times 20\times 20$ points was employed. There is a good agreement in the time scale of the response and in the intermediate and final average orientation of the director. In the lower right corner the time evolution of n in the middle of the roll is represented. In this particular point, where the secondary flow is null, the director exhibits the expected tumbling behaviour with the correct period ($\approx$1 s).

CONCLUSIONS

We have presented a numerical study of the nematodynamics in cylindrical Couette geometry. Adopting a suitable velocity profile we have taken into account the presence of rolling-like instabilities similar to those observed in Couette shear flow of common fluids at high shear rates. Due to the high

viscosity of our system, a lyotropic cholesteric polymer PBLG/m-cresol 14%, the onset of this secondary flow appears at low shear rates, as it has been widely proved by linear stability analysis and experimental evidences. The most relevant effect of the rolling instability on the director dynamics is to induce, after a short classical tumbling transient, a stationary distribution of the director with privileged orientations close to the shear plane.

Work is in progress to better define the nature of this secondary flow; in particular we aim at demonstrating that the roll formation derives from director fluctuations due to the presence of unbalanced elastic torques [26].

REFERENCES

[1] Ericksen, J. L. (1960). *Arch. Rat. Mech. Anal.*, *4*, 231; (1962). *ibidem*, *9*, 371.
[2] Leslie, F. L. (1968). *Arch. Rat. Mech. Anal.*, *28*, 265; (1979). *Adv. Liq. Cryst.*, *4*, 1.
[3] Coron, J. M. et al. (1991). *Nematics*, Kluwer Academic Publishers: The Netherlands.
[4] Chandrasekhar, S. (1992). *Liquid Crystals*, Cambridge University Press.
[5] Pieranski, P. & Guyon, E. (1974). *Phys. Rev. A.*, *9*, 404.
[6] Manneville, P. & Dubois Violette, E. (1976). *J. Phys.*, *37*, 285.
[7] Koch, A. J., Rothen, F., Sadik, J., & Schori, O. (1985). *J. Phys.*, *46*, 699.
[8] Barratt, P. J. & Manley, J. (1981). *J. Phys. D: Appl. Phys.*, *14*, 1831.
[9] Cladis, P. E. & Torza, S. (1975). *Phys. Rev. Lett.*, *35*, 1283.
[10] Barratt, P. J., Manley, J. M., & Nye, V. A. (1987). *Rheol. Acta*, *26*, 343.
[11] Polimeno, A. & Martins, A. F. (1998). *Liq. Cryst.*, *25*, 545.
[12] Polimeno, A.,Orian, L., Nordio, P. L., & Martins, A. F. (1999). *Mol. Cryst. Liq. Cryst.*, *336*, 17.
[13] Polimeno, A., Orian, L., Gomes, A. E., & Martins, A. F. (2000). *Phys. Rev. E*, *62*, 2288.
[14] Martins, A. F., Gomes, A. E., Polimeno, A., & Orian, L. (2000). *Phys. Rev. E*, *62*, 2301.
[15] Dunn, C. J., Ionescu, D., Kunimatsu, N., Luckhurst, G. R., Orian, L., & Polimeno, A. (2000). *J. Phys. Chem. B*, *104*, 10989.
[16] Martins, A. F., Gomes, A. E., Orian, L., & Polimeno, A. (2000). *Mol. Cryst. Liq. Cryst.*, *351*, 135.
[17] Larson, R. G. & Mead, D. W. (1993). *Liq. Cryst.*, *15*, 151.
[18] Callaghan, P. T. (1999). *Rep. Prog. Phys.*, *62*, 599.
[19] Martins, A. F., Esnault, P., & Volino, F. (1986). *Phys. Rev. Lett.*, *57*, 1745.
[20] Siebert, H., Grabowski, D. A., & Schmidt, C. (1997). *Rheol. Acta*, *36*, 618.
[21] De Gennes, P. G. & Prost, J. (1993). *The Physics of Liquid Crystals*, Oxford University Press.
[22] Taylor, G. I. (1923). *Philos. Trans. Roy. Soc.*, London, A223, 289.
[23] Chandrasekhar, S. (1961). *Hydrodynamic and Hydromagnetic stability*, Oxford University Press.
[24] Bird, R. B., Stewart, W. E., & Lightfoot, E. N. (1960). *Transport Phenomena*, Wiley.
[25] Fletcher, C. A. J. (1997). *Computational Techniques for Fluid Dynamics*, Springer Verlag: Heidelberg.
[26] Orian, L., Feio, A. G., Veron, A., Polimeno, A., & Martins, A. F., in preparation.